Deep-Sea Research II 103 (2014) 223–237

Contents lists available at ScienceDirect

Deep-Sea Research II

journal homepage: www.elsevier.com/locate/dsr2

# A climatology and time series for dissolved nitrate in the Gulf of Maine region

N.D. Rebuck [a,*], D.W. Townsend [b,1]

[a] NMFS/NEFSC/NOAA Narragansett Laboratory, 28 Tarzwell Drive, Narragansett, RI 02882, USA
[b] School of Marine Sciences, University of Maine, Orono, ME 04469, USA

ARTICLE INFO

Available online 20 September 2013

*Keywords:*
Nutrients
Nitrate
Water masses
Climatology
Time series
Gulf of Maine
Georges Bank

ABSTRACT

A compilation of data from 1932 to 2011 of dissolved inorganic nitrogen was used to generate spatially interpolated monthly climatologies for three depth layers in the Gulf of Maine region. Residuals from the spatial climatology are used to generate seasonal and annual time series. A bivariate co-kriging analysis was used to interpolate to a regular grid for each year within the historical record, then the resultant kriging error variance was used to determine a weighting value to generate the climatological mean. This interpolation method generates a realistic estimate as it incorporates most of the available nutrient data, geographic extrapolations based on defined spatial covariance functions, and an objective reproducible methodology. Residuals from the interpolated fields show the Gulf of Maine tends to vary on seasonal and annual timescales as a single cohesive unit, whereas intra-seasonal dynamics are more localized. Anomalies during the spring drawdown and fall replenishment are highly dependent on timing of the seasonal progression and less reliant on preceding nutrient conditions. Lagged correlations of residuals suggest seasonal mixing dynamics may be more important than elevated nutrient concentrations at depth to supplying surface waters with available nutrients.



## 1. Introduction

The Gulf of Maine and Georges Bank are historically important commercial fishing areas (Backus, 1987) and have been studied extensively in their physical and biological characteristics (Townsend et al., 2006). Dissolved nutrients and adequate light energy, along with top-down grazing, are primary determinants of photosynthetic productivity of the oceans. The primary nutrient limiting productivity in the Gulf of Maine region is nitrate (Kolber et al., 1990), with well-mixed and upwelling areas maintaining higher rates of productivity throughout the otherwise depleted summer months (Townsend et al., 2006). Other factors contribute to constraining phytoplankton populations, including grazing pressure (Durbin et al., 2003) and degree of vertical water column stratification (Ji et al., 2008; Song et al., 2010); however the input of dissolved inorganic nitrogen determines the extent of bottom-up control on productivity.

The high biological productivity of this region results from an influx of high concentrations of dissolved nutrients through seasonal mixing with sub-pycnocline waters and continuous tidal mixing that occurs coincident with unique bathymetric features labeled in Fig. 1, such as Georges Bank and the Bay of Fundy (Bigelow, 1927; Townsend et al., 2006). The offshore slope waters that provide about half of these nutrients (Townsend, 1998) derive from two sources: northerly Labrador Slope Water and southerly Warm Slope Water. The other half of the inflowing nutrients is brought by direct advection of waters from the Scotian Shelf during seasonal inflows from the northeast, in addition to localized freshwater river and continental inputs of terrestrial origin. This myriad of nutrient sources, in addition to seasonally varying uptake by phytoplankton, generate a complex and heterogeneous geographic and temporal distribution of biologically available dissolved nutrients.

The primary obstacle to producing a mean climatology from temporally disparate data is the inability to differentiate between persistent features of a substantially different mean state and aliasing due to low sampling frequency and poor spatial resolution. By combining observations from a limited set of years, it becomes numerically impossible to distinguish between geographical variability and interannual variability. Calculation of a mean state climatology is relatively straightforward when presented with sufficient data to eliminate geographic and temporal disparities. In field studies designed a priori, repeat stations are the easiest method to facilitate temporal averaging while retaining spatial homogeneity. Spatial averages generated by remote sensing and satellite measurements typically have high temporal resolution which can then be isolated into principal components for

* Corresponding author. Tel. +1 401 782 3240.
*E-mail address:* nathan.rebuck@noaa.gov (N.D. Rebuck).
[1] Tel.: +1 207 581 4367.

0967-0645/$ - see front matter 
http://dx.doi.org/10.1016/j.dsr2.2013.09.006

further evaluation of averages and influencing variables (Bisagni, 2003; Thomas et al., 2003). The nature of *in situ* water sampling and utilizing a historical database precludes many of the methods used by other data rich sources.

For example, repeated sampling at one location or mooring observations are spatially static and measure temporal variability. In contrast, a single satellite pass or isolated cruise minimizes temporal variability and measures only the spatial variability. A more complex situation is presented when data are spatially and temporally inconsistent, necessitating calculation and approximation to quantify each variable component and resolve the underlying mean condition. Dynamical modeling exercises often have difficulty resolving times of rapid transition such as the spring and fall phytoplankton blooms (Song et al., 2011; Anderson, 2009), suggesting a failure to capture important dynamics. To resolve these deficiencies and to incorporate the greatest number of *in situ* data in a realistic manner, an annually averaged multivariate simple co-kriging method was used to generate a monthly climatology of dissolved nitrate concentrations in the Gulf of Maine. Kriging itself is a method of optimal interpolation developed by Krige (1951) and refined further by Matheron (1963, 1965). Generally, the method is a least-squares interpolation of geographically irregularly sampled observations to the regularly gridded interstitial space, thereby calculating an estimate of values at any location near the sampled domain. While originally developed for temporally static geologic and earth science applications, the method can be used with appropriate selection of temporal windows and parameter weighting, and has been used in many fields that rely on spatial statistics such as oceanography, as well as meteorology, agriculture, and epidemiology (Carrat and Valleron, 1991).

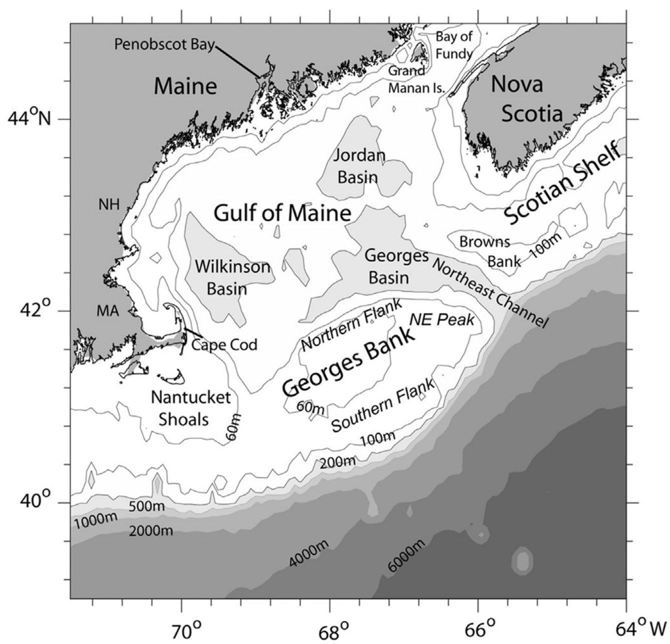


**Fig. 1.** Major bathymetric features and geographic areas of the Gulf of Maine and Georges Bank Region. Bottom depths are shown in meters. Figure from Townsend et al. (2014).

The climatology presented here consists of a Gauss-Markov map centered on three depth layers (1 m, 50 m, and 150 m) calculated for the midpoint of each month. The estimates were calculated by kriging available data for every month of every year, and then weighted averaging all available months based on the associated kriging error variance. Averaging in this fashion maximized the information available from each observation by extending its empirically supported geographic range through each monthly interpolation, but minimized the influence of less robust years through the weighted annual averaging. The resultant climatological maps produced estimates of nitrate concentrations, as well as the overall average kriging error that results from the calculation. This interpolation method highlights some of the persistent oceanographic features that influence the nutrient dynamics within the Gulf, as well as illustrates seasons and locations that lack extensive data coverage. Fig. 2 shows the geographic distribution of sampling in the region, with darker background colors indicating higher sampling density. As most programs are focused on the coastal zone or Georges Bank, the darkest shading covers those areas, while beyond the off-slope waters and the interior basins of the Gulf of Maine are less well sampled. The results of this climatology can be used in future modeling studies as an input variable or as output validation, as well as producing a yardstick to which future observations can be compared to describe relative nitrate abundance.

The climatology produced here is an extension both spatially and temporally over previous analyses conducted by repeated survey transects (Fournier et al., 1977), and earlier, temporally coarse interpolated works by Petrie et al. (1999) and Petrie and Yeats (2000). This analysis benefits from an extra 10 years of data

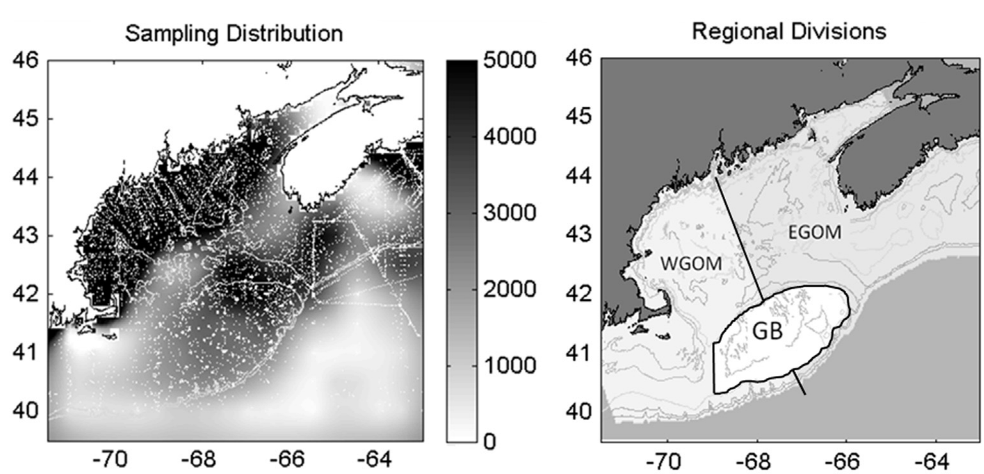


**Fig. 2.** Map of study area showing data distribution and regional divisions within the Gulf of Maine and Georges Bank region. Bathymetric contours are outlined, including the deep offshore basins, NE Channel, and shallow outer Georges Bank and Browns Bank. The sampling distributions (left) are shaded relative to geographic sampling density (number of samples per 0.5° bin), with individual samples highlighted in white. The regional areas isolated for analysis are Georges Bank (GB), Eastern Gulf of Maine (EGOM), and Western Gulf of Maine (WGOM).

accumulation, in addition to increased availability of historical observations consolidated in a central database (Boyer et al., 2009). Both previous gridding interpolations (Petrie et al., 1999, Petrie and Yeats, 2000) are based on Petrie and Dean-Moore (1996) who used a four parameter interpolation to calculate the variability in temperature and salinity seasonally as a proxy for nitrate, instead of the actual variance of nitrate used here. The length scales used here are slightly longer than those calculated by Petrie and Dean-Moore (1996), whereas the temporal scales are similar in surface waters but longer at 50 m and 150 m.

## 2. Methods

### 2.1. Historical data assemblage

The two primary sources for the data used in the analysis were the World Ocean Database (WOD, Boyer et al., 2009) and the Integrated Science Data Management of the Department of Fisheries and Oceans Canada (ISDM-DFO) in Ottawa (updated from Petrie et al., 1999). These two sources were combined with additional data that have remained in provisional or unreleased status and are listed in Table 1.

The quality control for the Gulf of Maine historical data is loosely based on that utilized by Conkright et al. (2002) and Johnson et al. (2009) for the WOD with adaptations for regional specificity. While nutrient analysis has undergone updates in methodology, comparison analyses show general agreement between contemporary automated and historical manual methods, with results falling within the experimental standard deviations at all but the lowest concentrations (Berberian and Barcelona, 1979; Airey and Sandars, 1987). Data were compiled into a standardized format of two decimal places for μM nitrate, and duplicates were eliminated with identical date, latitude and longitude, sample depth, temperature, salinity, and nitrate. Although some historical concentration values of zero have been incorrectly used as a "no data" placeholder and eliminated from early versions of the WOD (Conkright et al., 1994), zero concentrations were retained and eliminated only when they failed more recent WOD criteria (Johnson et al., 2009), when all corresponding macronutrient values (nitrate, silicate, and phosphate) were listed as zero, or when sampled below 40 m in depth.

One source of variability within the historical WOD and Petrie et al. (1999) datasets is the erroneous labeling as nitrate ($NO_3$) when measurements quantified the total dissolved inorganic nitrogen (DIN), which includes nitrate ($NO_3$), nitrite ($NO_2$), and ammonia ($NH_4$). Unfortunately, metadata for much of the historical measurements are unavailable (Johnson et al., 2009) and much of the historical data from Petrie et al. (1999) and the WOD are reported as solely nitrate. It is likely that most of the historical data labeled nitrate represent the sum of DIN, with a minority of measurements directly analyzing only the dominant component $NO_3$ (Conkright et al., 1994; Garcia et al., 2006; Boyer et al., 2009). When both nitrate and nitrite were provided in contemporary datasets, the sum of both was included under the assumption that the combined total was analogous to the older measurements lacking metadata. A regression of recent data that include separate nitrate and nitrite measurements generated a least squares linear fit with a slope of 0.03 and $R^2=0.39$. Of the data that contain a greater than average proportion of nitrite to nitrate, most occur in the vicinity of the Massachusetts Water Resource Authority (MWRA) effluent outfall field. As this small area represents a uniquely disturbed environment and is not representative of elsewhere in the region, any possible underestimation of nitrate via exclusion of nitrite in incorrectly labeled historical data is likely under 3% and therefore is negligible.

For initial quality control, data were binned into three categories: surface (0–39 m), intermediate (40–130 m), and deep (> 130 m). These depths were chosen to roughly approximate the prevalent seasonal water masses in the Gulf of Maine: Maine Surface Water (MSW), Maine Intermediate Water (MIW), and Maine Bottom Water/Slope Water (MBW) (Hopkins and Garfield, 1979; Townsend et al., 2006). The initial quality control eliminated samples that were > 4 standard deviations from the mean of each depth bin, slightly more stringent than the WOD global criteria of 5 standard deviations (Conkright et al., 1994). As four standard deviations below the mean extended into negative values, samples that were > 130 m and < 4 μM nitrate were also flagged as erroneous. This method resulted in removal of < 1% of surface nitrate samples and should be considered a conservative exclusionary criteria that errs on the side of inclusion. The resulting limits and percentage of observations flagged is shown in Table 2.

**Table 2**
Flagging criteria for raw data inputs. Depth bins for nitrate observations include surface (0–39 m), intermediate (40–130 m), and bottom (> 130 m), along with acceptable low range, acceptable high range, and percentage of samples flagged.

| Depth layer | Min $NO_3$ (μM) | Max $NO_3$ (μM) | Flagged (%) |
|---|---|---|---|
| Surface (0–39 m) | < 0 | 16.11 | 0.34 |
| Intermediate (40–130 m) | < 0 | 23.53 | 0.13 |
| Bottom (> 131 m) | 4 | 33.46 | 1.50 |

**Table 1**
List of data sources, years of collection, number of observations, and references to data locations for all data used in subsequent analyses. Most data is publicly available, either through published works or online. Data from the MWRA may have restrictions on some usage, while most other data is provided as preliminary, leading to the flagging criteria described.

| Program source | Acronym | Years | # Data | References |
|---|---|---|---|---|
| World Ocean Database | WOD | 1930–2010 | 49,551 | Boyer et al. (2009) |
| Massachusetts Water Resource Authority | MWRA | 1992–2009 | 31,597 | Werme et al. (2012) |
| Integrated Science Data Managment | ISDM-DFO | 1925–2005 | 30,661 | Petrie et al. (1999) |
| University of Maine | DWT | 1994–2011 | 18,248 | http://grampus.umeoce.maine.edu/nutrients |
| Woods Hole Oceanographic Institution | WHOI | 2003–2006 | 6478 | – |
| Gulf of Maine Toxicity Program | GOMTOX | 2007–2009 | 5827 | http://science.whoi.edu/users/olga/alex_surveys/Alexandrium_Surveys.html |
| NOAA NEFSC Marine Monitoring and Assessment Program | MARMAP | 1969–1982 | 5374 | Sherman (1980), Sibunka and Silverman (1984) |
| Atlantic Zone Monitoring Program | AZMP | 1999–2006 | 1893 | Therriault et al. (1998) |
| University of New Hampshire | UNH | 2004–2007 | 1481 | http://www.cooa.unh.edu/ |
| Gulf of Maine Regional Marine Research Program | RMRP | 1994–1996 | 1364 | http://gyre.umeoce.maine.edu/ |
| Sum raw inputs | | 1925–2011 | 152,474 | |
| **Total after QA/QC** | | **1932–2011** | 111,693 | |

### 2.2. Calculation of seasonal cycles

One difficulty in using kriging for a temporally variable set of data, such as a seasonally varying ocean, is the maintenance of first and second order stationarity. To normalize the seasonal mean, a harmonic was least-squares fit to the data plotted by yearday (days 1–365) for three separate areas within the greater region: Georges Bank (GB), Eastern Gulf of Maine (EGOM), and Western Gulf of Maine (WGOM), as shown in Fig. 2. Data were restricted to tighter depth ranges for the seasonal cycle and spatial interpolation analysis than the ranges used in quality control procedures, with surface restricted to 0–6 m, intermediate from 45–54 m, and deep waters as 145–154 m. A second order harmonic was fit to surface and intermediate levels, and a first order harmonic fit for data at 150 m. Higher order harmonics ( $>2$) have been shown to better reproduce seasonal phenomena in other physical parameters in the region (Smith, 1983), however temporal gaps in sampling lead to unrealistic fits and necessitated the lower order fits used here. Residuals from the seasonal cycle satisfy seasonal first-order stationarity. A harmonic was also fit to the seasonal cycle of standard deviation, also calculated per yearday. Only data within two standard deviations of the seasonal cycle within each area at each depth were retained in subsequent analyses. While data that fall outside of this range are likely reliable, utilizing only those near the seasonal average minimizes the effect of unusual outliers. Monthly interpolation was performed combining the seasonal cycle residuals with the seasonal average as calculated on the 15th of each month. Two methods were used to generate second order stationarity, or constant variance throughout the year. For the interpolation, only data used within a prescribed moving temporal window was used, thereby limiting the data to time periods where variance is similar. For the time series analysis, the residuals were normalized by the calculated seasonal cycle of the standard deviation of daily averages.

### 2.3. Objective analysis kriging methodology

The kriging method was used to generate monthly interpolations for each year within the data record (*e.g.* January 1981, January 1982, January 1983, *etc.*). The resulting individual monthly interpolations were then weight averaged to calculate the overall climatology. For each kriging interpolation, to retain some of the spatial discontinuities and fronts associated with persistent features, weighting parameters were generated from horizontal distance and the logarithm of bathymetry to incorporate some of the anisotropic but inconsistent natural variability. The regular interpolated gridded surface is 1/60th degree latitude and longitude, transformed to distance in meters using a Mercator projection giving an effective north–south latitudinal resolution of 1.37 km and a varying east–west longitudinal resolution between 1.77 km and 1.97 km. The corresponding bathymetry was supplied by the United State Geological Survey Gulf of Maine bathymetric grid (Roworth and Signell, 1999). The region was interpolated as isotropic and no effort was made to introduce boundary constraints; therefore interpolations are blind to landmasses and potential bathymetric isolation. While this may generate some error at the sparsely sampled deeper depths where the shape of bathymetric contours is more irregular (Lynch and McGillicuddy, 2001), the relatively consistent aspect ratio of the surface layers of the Gulf of Maine lends itself to this simplification.

The general kriging equation (Goovaerts, 1997)

$$Z^{*}(u)-m(u)=\sum_{\alpha=1}^{n(u)}\lambda_{\alpha}[Z(u_{\alpha})-m(u_{\alpha})]$$

where $u$ is the location vector, $n$ is the number of points used to interpolate, $m$ is the local mean, $\lambda$ is the kriging weight for each observation $\alpha$, and $Z$ being the variable of interest with $Z^{*}$ the interpolated estimate. Kriging assumes a constant first moment mean, thereby interpolating only the variance about the mean from each observation. At large scales with significant directional drift of the mean at each $u$, the mean is removed thereby interpolating only the residual deviation from the mean. The mean removed for the three areas shown in Fig. 2 was the seasonal cycle calculated in Fig. 3A.

### 2.4. Variogram weighting analysis

The most important choice when using the kriging method is the calculation of the weighting parameter $\lambda$. To achieve the best linear unbiased estimator for each gridpoint, an experimental variogram was calculated to determine the length and bathymetric scales of semivariance. The weights are calculated from an exponential model fit to the empirical variogram and then used to perform Gauss–Markov smoothing between the irregularly spaced observations to the structured grid (Gandin, 1965).

While each depth, season, and location potentially has different scales of correlation, incomplete sampling necessitates some compromise to provide consistency to the methodology. The weighting parameters were calculated via experimental variogram individually for each depth layer, approximating the three-layered model of waters within the Gulf of Maine (Bigelow, 1927; Hopkins and Garfield, 1979). The parameter weightings for each depth layer with respect to distance and logarithm of bathymetry are listed in Table 3. The interannual variability at 150 m was greater than the calculated seasonal cycle, therefore data from essentially the entire year are used to interpolate for each month. Bathymetry was not used at 50 m and 150 m as there was no consistent relationship with dissolved nitrate concentrations. The weighting function at each gridpoint is the exponential of the correlation scale multiplied by the square of the expected standard deviation within the monthly interpolated field. The monthly standard deviation was calculated from all data within each month, all years included.

### 2.5. Annual averaging of monthly fields

As the observations are samples from the true underlying mean, any calculation using the irregularly sampled data produces an estimate of the mean and some measure of the estimation's accuracy. As with any mean estimation, the number of observations increases the confidence in the estimate, and similarly the quality of the interpolation is highly dependent on the amount of data. While kriging is one method for producing the best linear unbiased estimator for a temporally static set of observations, the addition of temporal variability can produce biased estimates. To minimize this bias, kriging was used on timescales considered temporally static to produce multiple spatial interpolation, which were then averaged to generate the climatological average.

The kriging method provides a measure of the kriging error variance, calculated as the expected variance that results from the interpolation distance and the weighting scale. In using the exponential model to describe the geographic variance, kriging error variance in this interpolation increases rapidly beyond the prescribed distances in Table 3. Beyond the variogram range, the interpolated estimate reverts to the mean of all available data and kriging error variance reaches a maximum. To realistically average each available year into a multi-year climatological average, the individual monthly interpolations were averaged based on a weighted scale of the associated kriging error variance. As each calendar month for all years has the same maximum error variance, each monthly instance (*i.e.* per month, per year) was weighted such that the estimates with the lowest kriging error variance retained the highest weighting, and the maximum

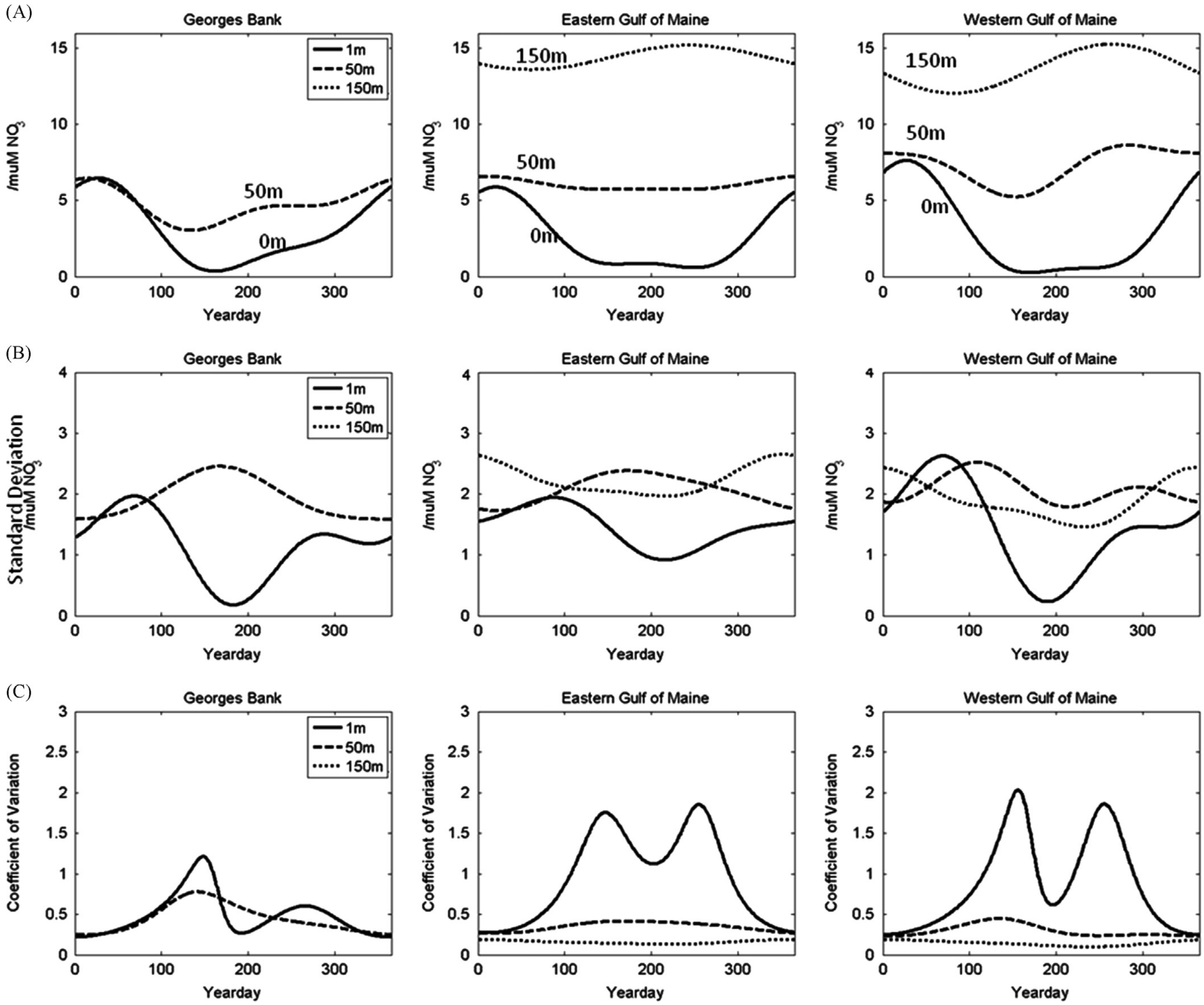


**Fig. 3.** Seasonal variation of dissolved nitrate concentrations for the three areas within the Gulf of Maine shown as (A) three panels across top, average seasonal cycle of nitrate concentrations, (B) three panels across middle, the seasonal progression of the standard deviation of nitrate concentrations and (C) three panels across bottom, the coefficient of variation based on the average and standard deviation shown above. The high coefficient of variation that occurs near the end of the spring bloom and beginning of the fall bloom highlight the importance of differentiating between factors that describe fluxes, such as winter or summer influences, and those merely reflecting a disconnect in timing, such as those in spring and fall.

**Table 3**
Weighting parameters for bivariate kriging interpolation modeled by an exponential fit of the experimental variogram. Bathymetry was only used in the surface analysis as variance was uncorrelated at the deeper depths.

| Depth (m) | Distance (km) | Temporal window (days) | Logarithm bathymetry (m) |
|---|---|---|---|
| 0 | 50 | 30 | 1 |
| 50 | 42 | 51 | – |
| 150 | 68 | 360 | – |

kriging error variance received a weighting of 0:

$$\lambda(u)_n = \frac{1-(\sigma_{max}/\sigma(u)_n)}{\sum_{n=year_{min}}^{year_{max}} 1-(\sigma_{max}/\sigma(u)_n)}$$

and the sum of annual weights equals to 1. This method ensures that estimations derived from nearby observations are given the most influence and those far from observations the least, while generating an estimate at all locations regardless of observational history. It also serves to smooth the edges and discontinuities that can result from discrete numeric thresholds and cutoffs in weighting.

### 2.6. Calculation of residuals and time series

To generate a time series from the observations, the monthly interpolated estimate was subtracted from the monthly midpoint residuals, *e.g.* the residuals from the areal seasonal cycle temporally corrected to the nearest monthly midpoint. This eliminates any temporal bias that may result from sampling early or late in any one month, and also eliminates any geographic bias by comparison to the spatially interpolated fields, describing only the interannual variability. To compare across seasons, the residuals were normalized by the fitted standard deviation in Fig. 3B.

Three methods were used to examine different phenomena: (1) variogram analysis of the normalized residuals to determine autocorrelation, (2) daily averages for the entire 1932–2011 dataset to examine intra-seasonal dynamics, and (3) seasonal bins of monthly averages which were also combined to generate a normalized annual average to examine interseasonal and interannual relationships. Seasons were calculated as the preceding December–February for the yearly winter, March–May as Spring, June–August for summer, and September–November for fall. All temporal scales were calculated at each of the three depths for each of the three regions shown in Fig. 2; the annual average seasonal series for comparison between depths was calculated as the average of all regions.

## 3. Results

### 3.1. Seasonal cycle

The initial calculation of the seasonal cycle shows the average dissolved nutrient concentrations in Fig. 3A, the average daily variability throughout the seasons in Fig. 3B, and the coefficient of variation (CV) throughout the year for each depth for the three areas throughout the Gulf of Maine region in Fig. 3C. The shallow GB has persistently lower surface and 50 m nitrate concentrations than the WGOM. Winter concentrations of nitrate are higher in the WGOM due to deeper winter mixing and stronger summer stratification. However, the dominant signal for all three regions is fairly consistent in timing and amplitude. Nutrient depletion occurs on average near day 150, or June 1st for all regions. In general the EGOM has a decreased seasonal cycle relative to the WGOM, most evident at 50 m.

The seasonal progression of variability, expressed as a curve fitted to the standard deviation for each day, shows the highly variable surface concentrations during the spring uptake and, to a lesser extent, the fall mixing and surface nutrient recharge. These patterns appear as the dual peaks in Fig. 3C, where the CV approaches 2 for the surface nitrate in the WGOM. The variability is much lower at 50 m and 150 m for the interior regions, however the variability at 50 m on GB is substantial during the spring bloom.

### 3.2. Average gridded products and spatial variability

The calculated climatological products for 1 m, 50 m, and 150 m are shown in Figs. 4, 6, and 8 respectively. The corresponding averaged kriging error variance maps are shown in Figs. 5, 7, and 9. The color scale is shifted seasonally for the surface interpolation in Fig. 4 for December–March (4–8 μM), April and November (0–4 μM), and May through October (0–2 μM) to highlight the geographic features within each month. Estimates are blanked seaward of the continental shelf (1000 m) where sampling is infrequent. Color scales at 50 m and 150 m are consistent throughout all months, and interpolations are blanked where bathymetry is shallower than the depth of interpolation.

As the kriging error variance is a function of both observation location and average *in situ* variability within each month, the color scale is shifted for the surface in Fig. 5 (Fig. 6), but is constant for 50 m in Fig. 7 (Fig. 8). The interpolation at 150 m was generated using a window of 360 days and the kriging error variance is equal for all months of the year, shown in Fig. 9. The error variance maps are not blanked corresponding with bathymetry, but instead show the entire interpolation domain.

### 3.3. Time series

The autocorrelation was determined by plotting an empirical variogram for the daily residuals and fitting the curve with an exponential function. The autocorrelation is defined as the range distance, or where the semivariance reaches approximately 95% of the maximum sill value (Cressie, 1990). The variograms for the surface and 50 m for the WGOM calculated that the semivariance approaches the maximum near 30 days in the surface, whereas at 50 m the semivariance increases slightly more gradually and approaches maximum near 51 days. Variograms constructed for GB and EGOM lacked any coherent structure as a result of inconsistent and incomplete sampling within the spatially heterogeneous areas. The WGOM area benefits from the inclusion of the MWRA dataset, which repeats sampling in fixed locations and is better positioned to describe the effects on shorter time scales.

For the daily record (1932–2011), surface nitrate concentrations were correlated between GB and EGOM ($r=0.23$, $p=0.0042$) but not for the other areas. At 50 m, the only correlation was between GB and WGOM ($r=0.26$, $p=0.05$); EGOM and WGOM were not correlated at 150 m. When restricted to the more reliable data from 1980 to 2010, the daily average correlations strengthened at 0 m for GB and EGOM ($r=0.35$, $p=0.0001$), no correlations existed at 50 m, and a negative correlation existed at 150 m ($r=-0.43$, $p=0.01$).

The seasonal anomalies showed much of the same pattern as the daily averages. Sequential seasonal surface nitrate concentrations were significantly correlated for GB and EGOM at $r=0.75$ ($p<0.0001$), EGOM and WGOM $r=0.38$ ($p=0.02$) while the relationship between GB and WGOM was more tenuous, $r=0.34$ ($p=0.08$). This pattern was repeated when isolating just the summer anomalies where all regions were correlated except GB and WGOM $r=0.45$ ($p=0.12$). There were no significant correlations in isolated autumn averages; winter anomalies were correlated GB to EGOM $r=0.65$ ($p=0.006$), GB to WGOM $r=0.44$ ($p=0.08$), and EGOM to WGOM $r=0.50$ ($p=0.04$). Spring anomalies were weakly correlated between GB and both EGOM and WGOM ($r=0.55$ and $r=0.45$, $p=0.04$ and $p=0.08$ respectively); however there was no correlation between EGOM and WGOM ($p=0.95$).

At 50 m, annual anomalies were correlated for GB and WGOM ($r=0.41$, $p=0.04$) and EGOM and WGOM ($r=0.49$, $p=0.004$), but not between GB and EGOM ($p=0.71$). None of the regions were correlated in summer, and only EGOM and WGOM were correlated in fall ($r=0.60$, $p=0.006$). Winter residuals were correlated for GB and EGOM ($r=0.80$ $p=0.005$) but not significantly for WGOM. Spring residuals were not correlated between areas. Residual anomalies at 150m were correlated between EGOM and WGOM when annually averaged ($r=0.43$, $p=0.05$) and for spring ($r=0.76$, $p=0.002$) and summer ($r=0.56$, $p=0.02$), but not for fall ($p=0.79$) and winter ($p=0.41$). The annual residuals for surface waters were autocorrelated to 2 years, but there was no significant relationship at a 3 year or greater lag. There was no significant autocorrelation of the annual averages at 50 m or 150 m.

Seasonal correlations between depths were highest in winter, with surface winter anomalies being significantly correlated to both 50 m winter anomalies and 150 m annual anomalies. There was a significant correlation between 50 m and 150 m as well. There was no significant correlation between winter 50 m anomalies and surface spring residuals, however there was a weakly significant correlation between 50 m winter residuals and 1 m summer residuals ($r=0.37$, $p=0.06$). A lagged correlation between 1 m winter residuals and 150 m annual anomalies had no significance beyond lag 0. The annually averaged residuals (not shown) are significantly positively correlated for all three depth layers.

## 4. Discussion

### 4.1. Methodological considerations

Several different methodologies were attempted to produce the climatology while retaining the information gathered in historical data as well as maintain the higher confidence in recent

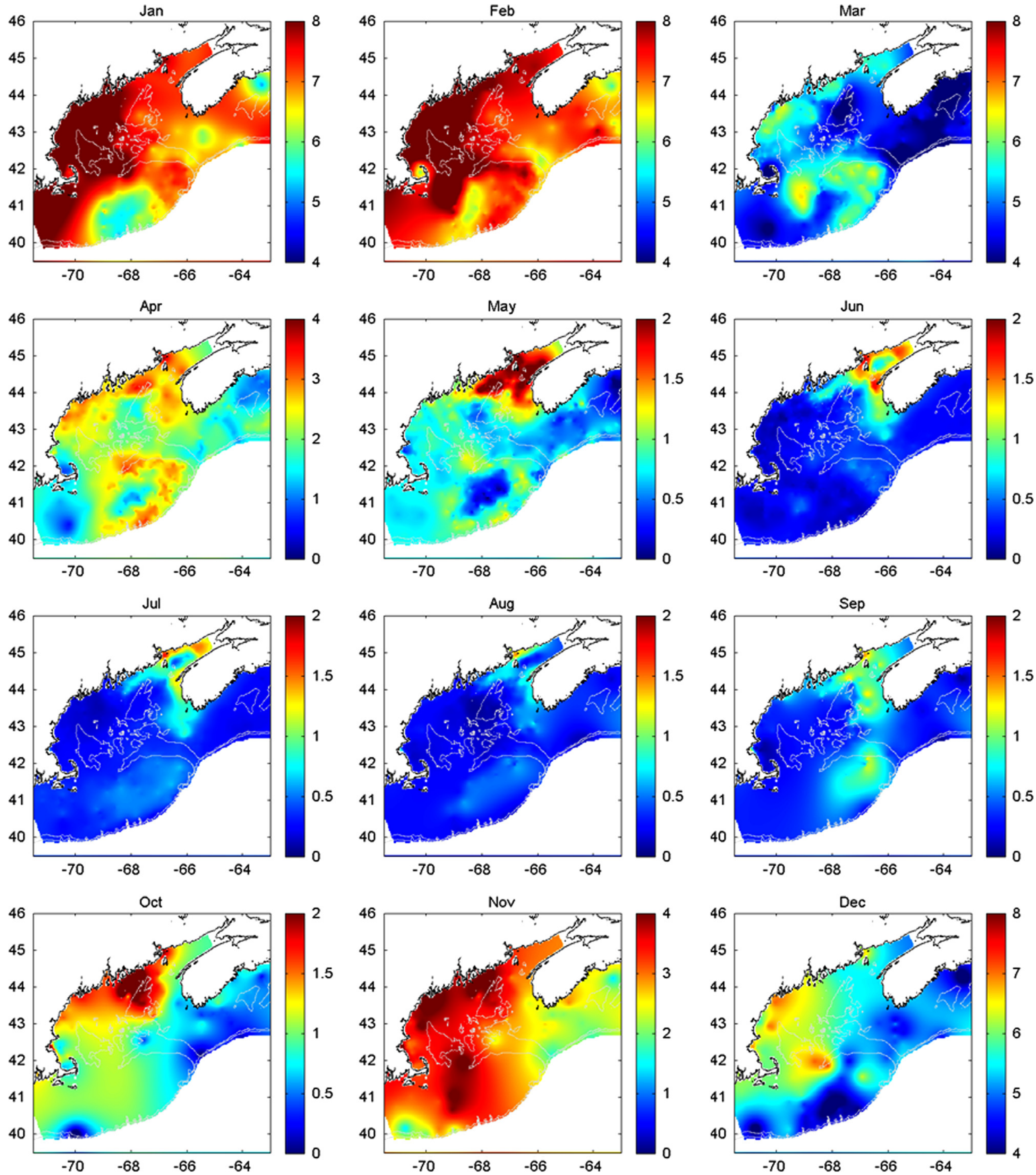


**Fig. 4.** Monthly climatology for nitrate (μM) in surface waters (0–6 m) for the Gulf of Maine. Color scales shift throughout seasons, however the seasonal cycle is clearly visible. Highest concentrations are in the western Gulf of Maine in January and February, with depletion readily apparent throughout the summer months.

measurements. Data were not sufficient for principal component analysis, as frequently applied in satellite remote sensing (Thomas et al., 2003). An attempt was made to incorporate only the highest confidence estimates via retaining those of lowest kriging error variance similar to that conducted by Rohde et al. (2013), however the resultant estimates were plagued by unrealistic frontal boundaries resulting from the methodology. Remnants of this effect are present in this analysis, most notably in the surface layer in September, where frontal zones can be seen uncorroborated with any mechanistic underpinning. To produce a more realistic average field, the data must either be truncated, possibly ignoring useful information, or extrapolated using available proxy measurements. The final product here balanced between these two extremes, by averaging the interannual variability where warranted to smooth frontal boundaries while not estimating conditions were doing so is not warranted.

The selection of grid sizes, both temporally and spatially, was driven by several factors. The ~30 days month was based on a

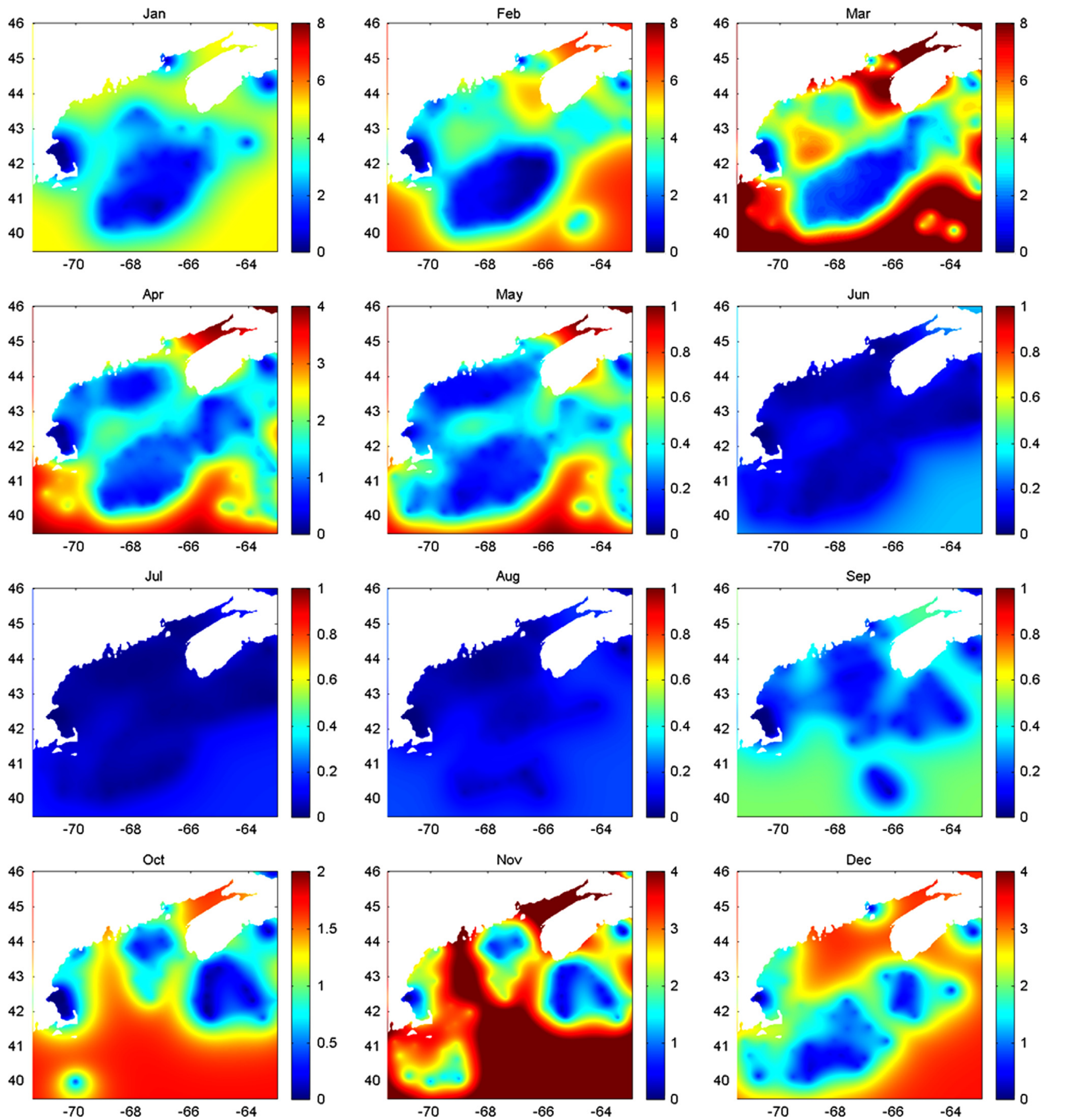


**Fig. 5.** Kriging error variance for the monthly climatology for nitrate (μM) in surface waters (0–6 m) for the Gulf of Maine. Color scale shifts throughout seasons. Heavily sampled regions and times have lower variance, such as Georges Bank and the entire domain during summer months. Offshore variance is typically high where sampling is light.

non-stationary variogram analysis that shows nitrate concentrations are correlated near 0.80 at 30 days and typically occur before the sharp divergence generated by the seasonal cycle. The temporal grid spacing is ultimately a balance between resolution and kriging error. Previous seasonal climatologies (4 interpolations per year) have been produced using only a fraction of the data available here (Petrie et al., 1999; Petrie and Yeats, 2000), resulting in an equivalent error variance but at the cost of temporal resolution. While some of the modeled fields presented here have areas of high kriging error variance, most notably some of the winter months, this resolution provides the ability to better describe the localized variability that occurs between the monthly and seasonal timescale. While the temporal grid is spaced evenly for comparison, future analyses could include a temporally variable grid to better balance the error variance to resolution ratio.

Similar to the selection of the temporal resolution, the horizontal grid spacing is a compromise between resolution and kriging error variance. A larger grid spacing would necessarily include more direct observations and smaller distances to estimation points, however feature identification would decrease in sensitivity. While this may decrease the magnitude of the kriging

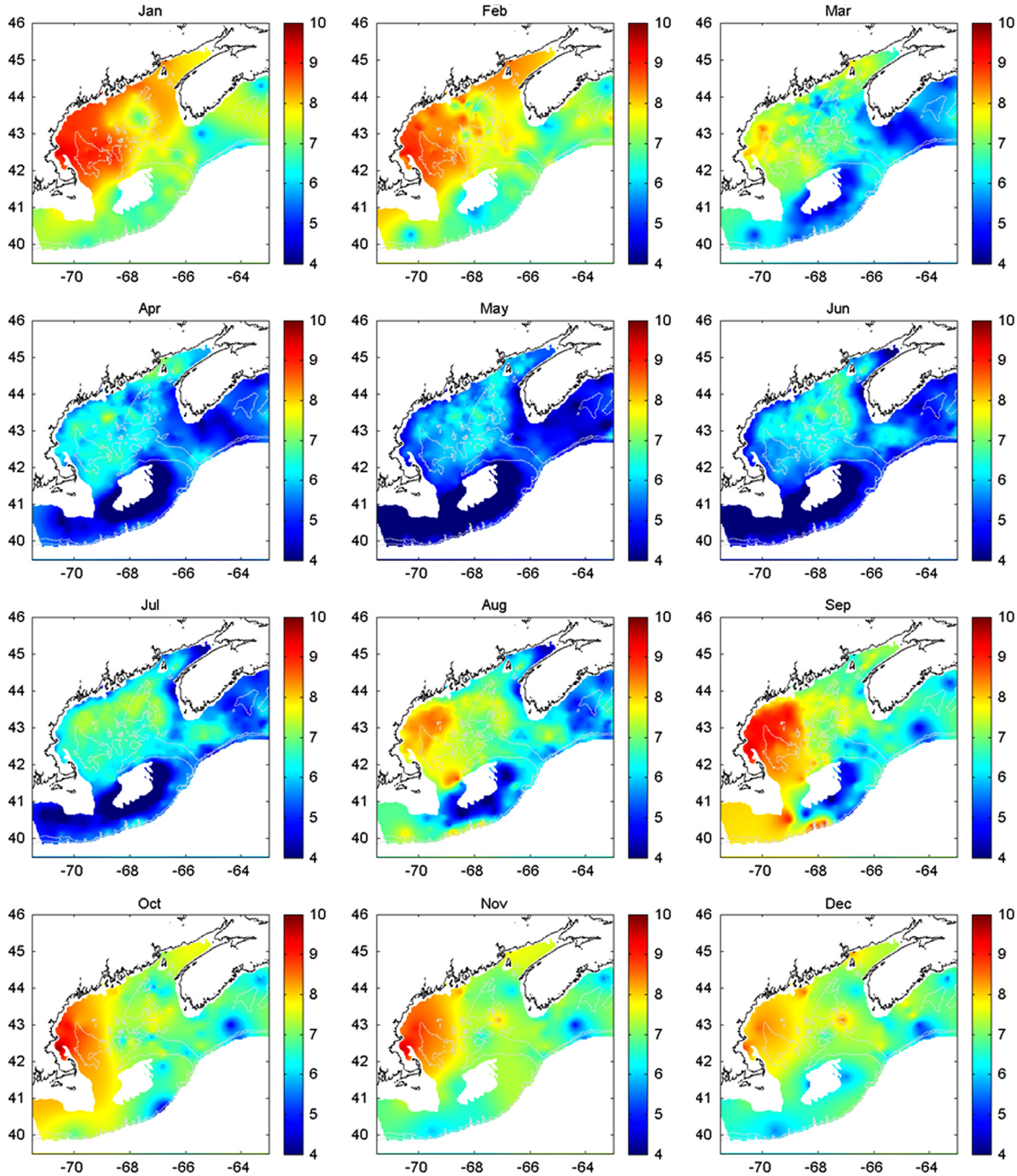


**Fig. 6.** Monthly climatology for nitrate (μM) in intermediate waters (45–56 m) for the Gulf of Maine. Areas of water depth <50 m and >1000 m are blanked (white). The seasonal cycle is still apparent at 50 m, however nitrate is never fully depleted in interior eastern regions as it is on Georges Bank.

error variance, it would also produce a more smoothed monthly estimation of nutrient concentrations.

Variations of the kriging method have been developed where high degrees of precision are necessary to describe a system with low global variance, small measurement error, and a high density of observations (Cressie and Kang, 2010; Meng et al., 2010). As the nugget values from temporal experimental variograms ranged from 0.80 $\mu M^2$ at the surface for daily binned data and up to 2.20 $\mu M^2$ at 150 m, the precision achievable by the interpolation using the currently available data is similarly blunted and subject to inevitable sub-gridscale variability.

Determining the best linear unbiased estimator using the kriging method is contingent on input observations being second order stationary or, more commonly, satisfying the intrinsic hypothesis. Second order stationary is satisfied if the covariance between observations is dependent only on the distance between them, whereas the intrinsic hypothesis is similar but uses the covariance of the first order differences, $Z(x+h)-Z(x)$ to determine the

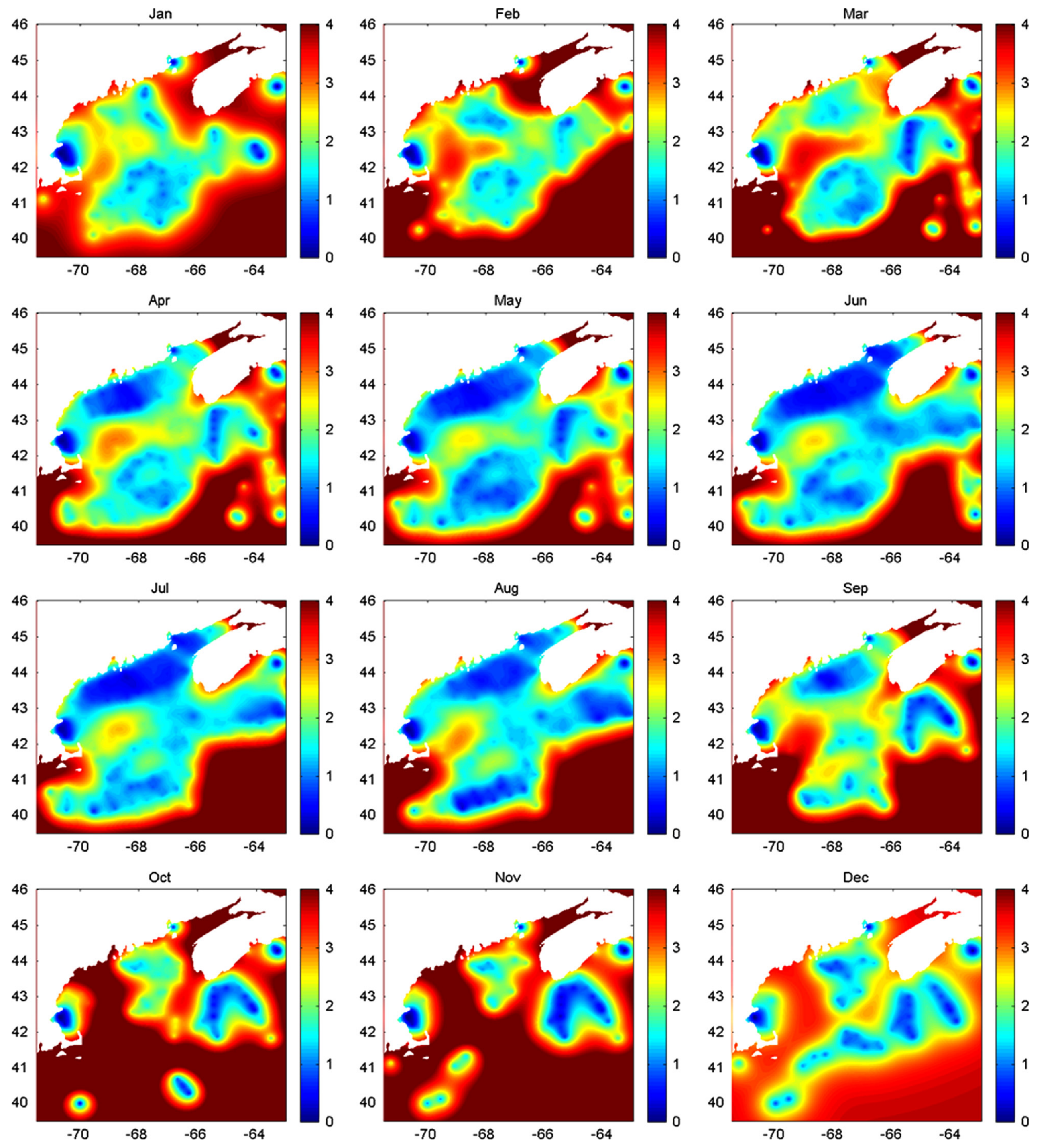


**Fig. 7.** Kriging error variance for the monthly climatology for nitrate (μM) in intermediate waters (45–56 m) for the Gulf of Maine. The coastal region is well sampled, and the MWRA sampling location between Cape Cod and Cape Ann is visible in all months as a steady patch of blue. As this data is not bathymetrically blanked, shallow inshore areas, and the crest of Georges Bank, appear as relatively higher in error variance.

covariance between observations (Myers, 1989). In dynamic environments that constantly vary in space and time, such as the marine nutrient environment, the stationarity of the nutrient concentrations is not strict but is typically adequate across relatively homogenous domains, such as the nutrient replete conditions at the surface in winter or below the seasonal thermocline.

In some instances, the underlying nutrient distribution as a function of spatial location may not be stationary, second order stationary, or satisfy the intrinsic hypothesis. In such instances it is typical to assume the underlying function to be weakly stationary with a degree of drift, such that $Z(x)=Y(x)+m(x)$, where $m(x)$ is the varying mean condition which is removed prior to calculation of the semivariogram and kriging interpolation. In a multi-dimensional analysis of a spatially heterogeneous environment, such as this one, there are several obstacles to achieve stationarity of the observations.

One complication of removing a trend, $m(x)$, is that the underlying function of nitrate concentration, *e.g.* the spatially and temporally variable mean, is precisely the desired result of the kriging analysis. If the background mean condition were known, the calculation would be superfluous. Typically, the data are used to provide a reasonable estimate of any trends in the underlying

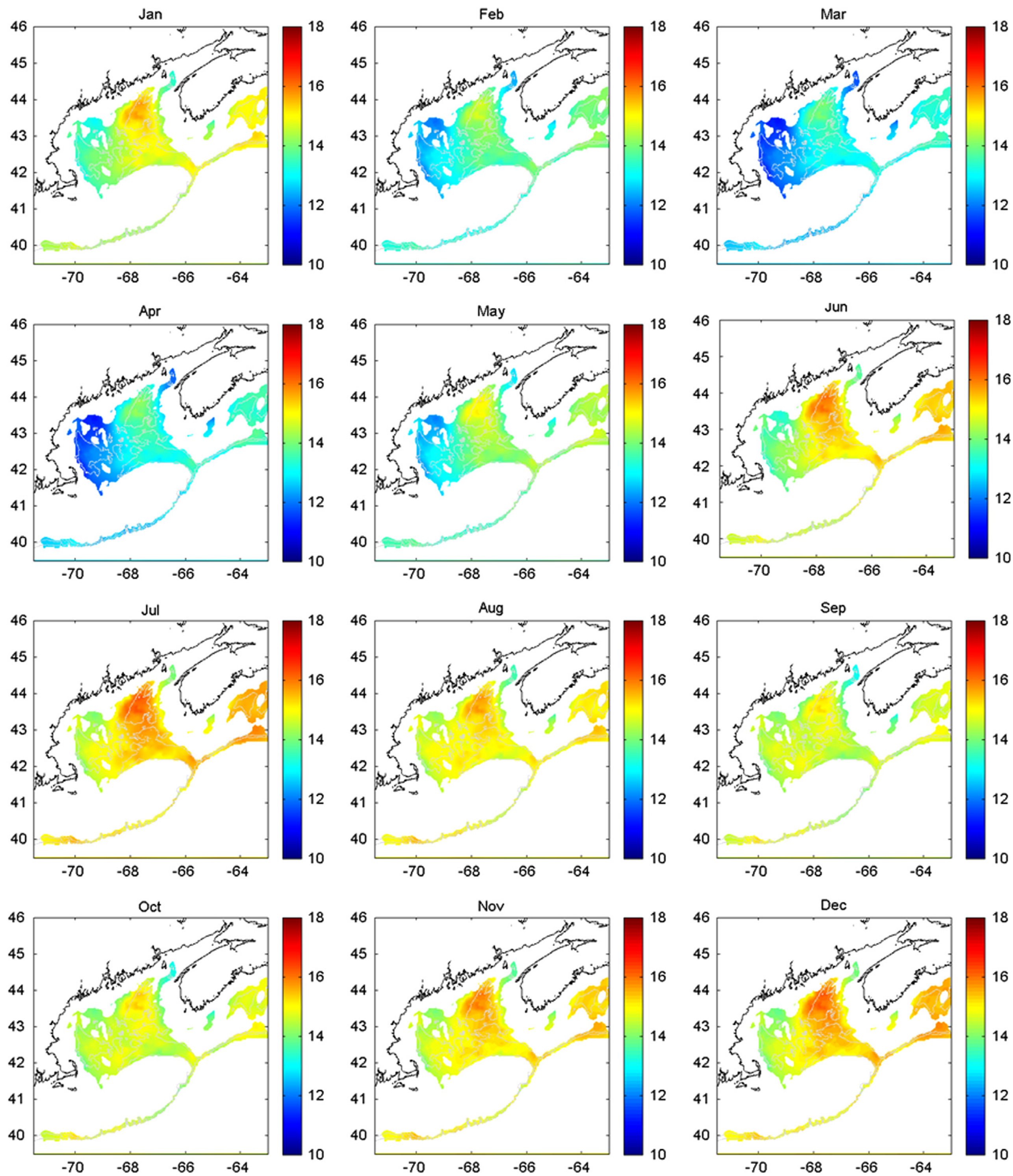


**Fig. 8.** Monthly climatology for nitrate (μM) in bottom waters (145–156 m) for the Gulf of Maine. There is some seasonality, particularly for the more western Wilkinson Basin, but overall concentrations remain elevated throughout the year.

function (Clark, 2001), however the complicated geometry and bathymetric influence of nitrate concentrations at the surface complicate the function beyond a simple linear trend. Estimated mean fields from prior studies could be used, however for this region the best estimates to date are calculated on a seasonal timescale and with larger grid spacing, possibly generating unrealistic patterns based on incomplete data.

An artificially generated estimate of the underlying mean field necessarily introduces some form of bias to the calculation. As the kriging procedure conducted on observations that are stationary with a drift is conducted on the residuals, $Y(x)$, the drift function, $m(x)$, is added to the kriged fields of variance to generate the estimated value. Therefore inserting an inaccurate estimation of the underlying spatial function can generate subjective and

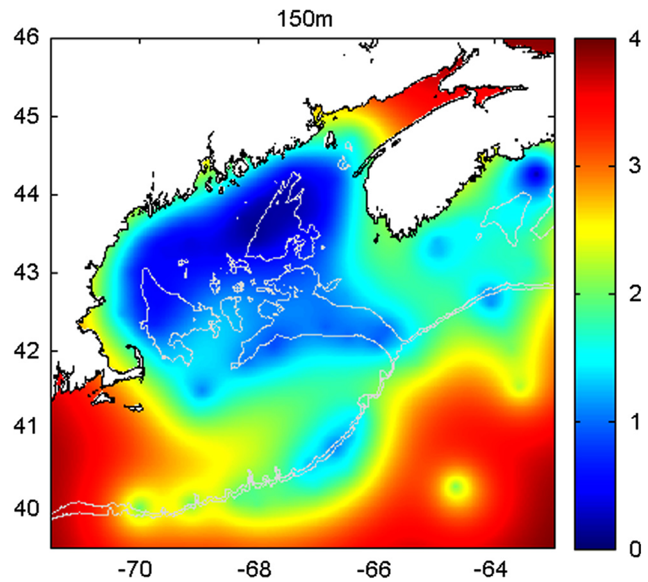


**Fig. 9.** Error variance for nitrate (μM) climatology at 150 m. As each monthly interpolation includes observations from the entire year and varies only in the mean seasonal cycle, the error variance for each month is identical. Monthly variations in the estimate arise from re-insertion of the seasonal cycle in both the western and eastern Gulf of Maine. Without data blanked < 150 m, the blue areas are those within the weighting distance of observations. The shaded contours are for 200 m depth.

artificial features not supported by the data. The approach used here assumed a spatially consistent underlying mean function for three areas within the domain for each monthly interval in attempts to draw the greatest information from the *in situ* data without being influenced by external bias. While this is a reasonable assumption at intermediate and deep depths that are less influenced by biological processes, photosynthetically influenced surface concentrations suffer from a tendency to remove gradients and fronts. Future iterations may benefit from the results of this work to better ensure geographic stationarity.

### *4.2. Seasonal cycle*

The seasonal cycles in Fig. 3A are typical for a mid-latitude shelf sea and highlight the dominance of surface production to the nitrate seasonal cycle. The general seasonal cycle trends and amplitudes correspond well to those described in Bisagni (2003), however the more numerous data used here provide a more complete description of the interannual variability. As noted in the Bisagni (2003) analysis, the spring and fall transitions occur rapidly, and slight shifts in the timing of these events, when averaged, smooth these transitions. As the variability in concentrations in the EGOM can equal 200% of the mean at the surface and 50% of the mean at 50 m calculated in Fig. 3C, this may partially account for the nutrient flux deficit calculated for the EGOM in the Bisagni (2003) study. The lower amplitude cycles in the EGOM in Fig. 3A show the influence of tidal mixing and decreased stratification, which allow nutrients to remain elevated at 50 m while remaining decreased at the surface. Interestingly, these same two mechanisms are at work on Georges Bank, where 50 m nitrate is decreased substantially relative to the EGOM. The shallower bathymetry on the offshore bank typically generates increased productivity through increasing light availability, likely accounting for the difference between the two regions, as well as isolating waters at 50 m from both deeper and horizontally advected nutrient sources.

The variability in nitrate, calculated as the daily average standard deviation and coefficient of variation, highlights the importance of phenology when calculating nutrient residuals. The dual peaks of surface CV evident in Fig. 3C are a result of the high variance compared to lower mean concentrations at the end of the spring drawdown and beginning of fall overturn. This variability highlights the difficulty in describing an entire year as high or low in nutrient concentrations. For example, a strong early winter with deep vertical mixing may generate a positive anomaly in the surface waters, however a relatively calm late winter/early spring may initiate an early bloom and generate substantially lower residuals than expressed during the winter months due to the rapid rate of change during that time. This was one of the primary reasons the time series were examined on a seasonal basis, with the expectation that winter and summer residuals would reflect more meaningful relative minima or maxima in terms of absolute concentrations, whereas spring and fall residuals would be influenced by the timing of the transitions.

At 150 m, the highest annual concentration appears near day 250 for both areas. This is slightly later than reported by Petrie and Yeats (2000), who found highest deep nutrient concentrations in summer. However the maximum near yearday 250 and minimum near day 50 corresponds roughly the seasonal cycle for temperature in the offshore basins, potentially reflecting vertical mixing down to 150 m. On average, EGOM has a higher average nutrient concentration than the WGOM, consistent with its location closer to inflowing, high-nutrient slope water sources (Schlitz and Cohen, 1984), fewer losses due to sediment denitrification (Christensen et al., 1995), and greater stratification leading to less vertical mixing with surface waters (Brown and Beardsley, 1978; Mountain, 2004).

### *4.3. Spatial and temporal variations in the interpolated products*

The most prominent bathymetric feature in the Gulf of Maine region is the shallow offshore Georges Bank. This area has been the focus of intense study (Wiebe et al., 1996) and at one time was the source of large commercial catches of cod and other groundfish (Backus, 1987). Georges Bank, along with the smaller Browns Bank to the north, serve as the major obstacles to water exchange between deep offshore sources and the interior Gulf of Maine (Townsend et al., 2005). The clockwise circulation produced by tidal flow on the bank (Loder, 1980) and intensified by vernal stratification (Naimie, 1996) produces an isolated mass of water on the crest of the bank resistant to off-bank mixing. This physical isolation leads to increased nitrogen limitation and recycling (Townsend and Pettigrew, 1997) on the crest of the bank. This pattern is evident in the surface layer nitrate concentrations in Fig. 4, showing nitrate levels on the crest of the bank reduced relative to the surrounding deeper areas during many months of the year and most noticeable from April through June. Surrounding the crest, the tidal mixing on the edges of the bank provide increased nitrate to the surface in all months, especially March through May, with the most noticeable area of increase on the northeast peak of Georges Bank.

The other noteworthy persistent feature is the coastal current, stretching from the tidal mixing on Browns Bank off the southeast coast of Nova Scotia, proceeding counter-clockwise through the Bay of Fundy, and continuing southwestward along the coast of Maine, with bathymetric features labeled in Fig. 1. While less noticeable during the high-nutrient winter months, during periods of nutrient depletion from April to November, the coastal current appears as a band of increased concentration hugging the coast of the eastern Gulf of Maine. Primarily driven by differential densities of the well mixed coastal waters and offshore sources (Xue et al., 2000; Pettigrew et al., 2005), the coastal current stretches from the southern tip of Nova Scotia across the Bay of Fundy where the highest nutrient injection to the surface occurs just southwest of

Grand Manan Island, where surface concentrations rarely fall below 2 μM $NO_3$.

The preliminary examination of the modeled surface nitrate concentrations reveals general agreement with the commonly recognized oceanographic features within the Gulf of Maine, such as Georges Bank and the coastal current described above, in addition to the highest surface nitrate concentrations in Wilkinson Basin in the late winter months (Townsend and Pettigrew, 1997) coincident with the coldest temperatures and greatest vertical mixing (Bigelow, 1927). Throughout the surface layers, the annual pattern is similar with a relatively rapid drawdown beginning in March and remaining decreased through September, followed by a increase in nitrate concentrations in October and November. As this process is likely event-driven by storms which degrade stratification, the climatology likely underestimates the rate at which nutrients are replenished and instead smoothes all events into a more continuous gradation.

Maine Bottom Water found in the deep offshore basins has been described as modified slope water (Bigelow, 1927; Hopkins and Garfield, 1979; Mountain and Jessen, 1987). The two dominant sources of this slope water are Warm Slope Water (WSW) of southern origin and Labrador Slope Water (LSW) of a northern origin. These two water masses have been described as the modal states of bottom waters in the Gulf that are correlated on a decadal scale with the North Atlantic Oscillation (NAO; Smith et al., 2001; Greene and Pershing, 2003). Typically, a high NAO corresponds to a prevalence of WSW and a negative NAO correlates with more LSW. A limitation of a constructing a mean climatology for the Gulf of Maine involves the averaging of the two modal states that may not accurate reflect the expected conditions.

In addition to each having a distinct temperature and salinity signature, each slope water type carries different nutrient loads that reflect the age and history of its source. WSW is older and contains nitrate concentrations near 25 μM, whereas the younger LSW contains nitrate concentrations closer to 15 μM (Drinkwater et al., 2002; Petrie and Yeats, 2000; Townsend et al., 2006; Townsend and Ellis, 2010). While both sources are subject to similar tidal and convective mixing processes that modify the original concentrations once inside the Gulf of Maine, an average value of the two will not accurately represent the true conditions except during a modal state transition. As the majority of the nutrient observations used here come from the dominantly NAO positive state from 1970 to present, this climatology likely reflects the elevated nutrient concentrations of WSW, which may or may not reflect the most common condition on a longer ( $>50$ year) timescale.

### 4.4. Time series considerations

Evaluation of the autocorrelation and cross-correlation between areas and seasons was highly sensitive to the temporal averaging method used, reflecting the inconsistent historical sampling. For the daily averages, the time series was frequently disjointed and contained relatively few instances where all three areas (GB, EGOM, and WGOM) were sampled concurrently. While this method retained the highest temporal resolution, the lack of data coverage affected the statistical power to compare between regions. The monthly averages, which were then combined into seasonal and annual averages, produced the most complete series, but lack the sensitivity to identify intra-seasonal dynamics.

The seasonal and annual correlations show that in general the Gulf of Maine region varies as a single unit as suggested by Bisagni (2003), with Georges Bank and the eastern Gulf of Maine being more correlated in seasonal surface residuals than the western area. This is similar to the EOF analysis of chlorophyll calculated in Thomas et al., (2003), in which the two dominant modes were geographically similar throughout the region. In that same analysis, the third component, which described 8.14% of the variance, showed an opposite signal for Georges Bank and southern areas relative to northern areas. These areas were isolated by using a similar EOF in Bisagni (2003), however the *in situ* data available in each region then became sparse and lacked a well defined description of the variability within each area. This analysis captures the variability within each region, but as our divisions between eastern and western areas was described as a line running from northwest to southeast, it may have diluted those differences in the two interior Gulf of Maine areas.

The annually averaged autocorrelation in surface waters was significant at lags of 1 and 2 years, yet Brown and Beardsley (1978) calculated the flushing time of the Gulf of Maine to be one year or less. Along with the absence of any significant lagged correlations at deeper depths, this temporal mismatch suggests that the forcings that affect surface nutrient concentrations can be as important in determining concentrations as the source waters themselves. The role of broader multi-year atmospheric variability, such as the NAO, has been described in terms of its impacts to variability in water mass dynamics (Smith et al., 2001; Greene and Pershing, 2003; Mountain, 2012), but little oceanographic research has investigated the role of these climate indices on the physical mechanisms of mixing and stratification in the Gulf of Maine. While decadal scale shifts of inflowing slope waters certainly alter the nutrients within the Gulf (Townsend et al., 2010), it may be the annual local processes that ultimately determine the concentrations of deep nutrients that become photosynthetically available at the surface. This is not absolute, however, as positive correlations exist between surface residuals and those at 50 m and 150 m, which implies that high nutrients at depth do translate to higher nutrients at the surface to some degree. It is more likely that the presence of high nutrients at depth provides a greater probability of elevated nutrients, and possible elevated productivity, but local mixing processes are required to realize any nutrient gains.

## 5. Conclusion

The incorporation of a multi-decadal dataset provides realistic estimation of the climatological average for the sampled history of nitrate for the Gulf of Maine, although it may be slightly skewed towards conditions more prevalent in the most recent 1990s and 2000s decades. Approaches that rely on dynamic models of biological phenomena often generate expected outcomes and do not necessarily describe the *in situ* conditions, particularly for poorly understood phenomena such as the fall bloom. The statistical model presented here incorporates nearly the entire historical record of nitrate in the region. As data inventories grow and the potential temporal and spatial resolution increases, periodic re-evaluation of the mean state will provide further insights into the nutrient dynamics of the Gulf of Maine. Deviations from the mean state calculated here can also identify decadal-scale shifts in available nutrients, potentially affecting the primary production and trophic structure within the region.

This analysis generates a climatology that builds upon those produced previously (Garside et al., 1996; Petrie et al., 1999; Petrie and Yeats, 2000), and future attempts should continue to better identify and account for the underlying trend surface. The approach used here partially accounts for a spatially variable but unknown mean (Armstrong, 1984); future efforts including increased data density may enable the use of other techniques to account for the mean, such as universal kriging (Matheron, 1969). Despite the inherent limitations of temporally and spatially scattered data, this interpolation presents the first objectively analyzed monthly-scale nutrient field derived solely from *in situ* data. As such, it can be considered an initial development that could be used in the future when an independent estimation of the mean function is desired.

The objective of the kriging method is to produce the best linear unbiased estimate from the available observational data to the prescribed model grid (Cressie, 1990). While the resulting estimate is the best available from the data, there is no assurance that it accurately describes the true underlying function, in this case the average nitrate concentration in each month. Further sampling during poorly represented periods and during opposing modal states, such as the slope water shifts manifest in the bottom waters (Smith et al., 2001; Greene and Pershing, 2003), is necessary to more completely describe the nitrate variability in the Gulf of Maine. Equally important, the further use and applicability of this or any future kriging interpolation must be coordinated with the desired product, whether it be a description of the mean underlying function, identification of spatial and temporal variability from the mean, or identification of poorly sampled areas and seasons.

## Acknowledgments

The work reported here was only possible with the help of many individuals and institutions who have over the years contributed their nutrient and hydrographic data to the various databases used in this study. It is a testament to oceanographers, marine chemists, and laboratory analysts everywhere that the original data from N.R. Rakestraw in 1932 can contribute to science 80 years after collection. We also need to acknowledge the generous assistance from individuals who willingly compiled and shared data and engaged in useful and stimulating discussions, including Dennis McGillicuddy, Brian Petrie, Jon Hare, Maureen Taylor, and Neal Pettigrew. Special thanks go to Maura Thomas, who personally has analyzed more nutrient samples from the Gulf of Maine than anyone, and to Keston Smith for assistance in developing functional programming. Funding was provided by grants from the National Science Foundation and the National Oceanic and Atmospheric Administration, Grant no. NA06NOS4780245 for the Gulf of Maine Toxicity Program (GOMTOX), the University of Maine Chase Distinguished Research Assistantship, and the National Research Council Post-doctoral Associateship. This is ECOHAB contribution no. 762.

## References

Airey, D., Sandars, G.A., 1987. Automated Analysis of Nutrients in Seawater. CSIRO Marine Laboratory Report 166, 95 pp.
Anderson, L.A., 2009. The seasonal nitrogen cycle in Wilkinson Basin, Gulf of Maine, as estimated by 1-D biological model optimization. J. Mar. Syst. 78, 77–93.
Armstrong, M., 1984. Problems with universal kriging. Math. Geol. 16 (1), 101–108.
Backus, R.H. (Ed.), 1987. Georges Bank. MIT Press, Cambridge, Massachusetts.
Berberian, G.A., and Barcelona M., 1979. Comparison of manual and automated methods of inorganic micro-nutrient analysis. NOAA Technical Memoranda ERL AOML 40, 26 pp.
Bigelow, H.B., 1927. Physical oceanography of the Gulf of Maine. Bull. U.S. Bur. Fish. 40 (II), 1015–1027.
Bisagni, J.J., 2003. Seasonal variability of nitrate supply and potential new production in the Gulf of Maine and Georges Bank regions. J. Geophys. Res. 108 (C11), 8015–8037.
Boyer, T.P., Antonov, J.I., Baranova, O.K., Garcia, H.E., Johnson, D.R., Locarnini, R.A., Mishonov, A.V., O'Brien, T.D., Seidov, D., Smolyar, I.V., Sweng, M.M., 2009. World Ocean Database 2009. Levitus, S., (Ed.). NOAA Atlas NESDIS 66, US Gov. Printing Office, Washington DC, 216pp., DVD.
Brown, W.S., Beardsley, R.C., 1978. Winter circulation in the Western Gulf of Maine: Part 1. Cooling and water mass formations. J. Phys. Oceanogr. 8, 265–277.
Carrat, F., Valleron, A.J., 1991. Epidemiologic mapping using the "kriging" method: application to an influenza-like epidemic in France. Am. J. Epidemiol. 135 (11), 1293–1300.
Christensen, J.P., Townsend, D.W., Montoya, J.P., 1995. Water column nutrients and sedimentary denitrification in the Gulf of Maine. Cont. Shelf Res. 16 (4), 489–515.
Clark, I., 2001. Practical Geostatistics. Geostokos, Scotland, UK.
Conkright, M.E., Levitus, S., Boyer, T.P., 1994. World Ocean Atlas, vol. 1. Nutrients. National Oceanic and Atmospheric Administration, Wash., D.C. p. 150.
Conkright, M.E., Locarnini, R.A., Garcia, H.E., O' Brien, T. ,Boyer, T.P., Stephens, C., Antonov, J.I., 2002. World Ocean Atlas 2001: Objective Analyses, Data Statistics, and Figures, CD-ROM Documentation, NODC Internal Report 17, Silver Spring MD, 17 pp.
Cressie, N., 1990. The origins of kriging. Math. Geol. 22 (3), 239–252.
Cressie, N., Kang, E.L., 2010. High-resolution digital soil mapping: kriging for very large datasets. In: Viscarra-Rossel, R., McBratney, A.B., Minasny, B. (Eds.), Proximal Soil Sensing. Springer, Dordrecht, 49–63.
Drinkwater, K.F., Petrie, B., Smith, P.C., 2002. Hydrographic variability on the scotian shelf during the 1990s. NAFO SCR Doc. 02/42, 16pp.
Durbin, E.G., Campbell, R.G., Casas, M.C., Ohman, M.D., Niehoff, B., Runge, J., Wagner, M., 2003. Interannual variation in phytoplankton blooms and zooplankton productivity and abundance in the Gulf of Maine during winter. Mar. Ecol. Prog. Ser. 254, 81–100.
Fournier, R.O., Marra, J., Bohrer, R., Van Det, M., 1977. Plankton dynamics and nutrient enrichment of the Scotian Shelf. J. Fish. Res. Board Can. 34, 1004–1018.
Gandin, L.S., 1965. Objective analysis of meteorological fields. Isr. Prog. Sci. Transl. vi., 242.
Garcia, H.E., Locarnini, R.A., Boyer T.P., Antonov J.I., 2006. World Ocean Atlas 2005, vol. 4. Nutrients (phosphate, nitrate, silicate). Levitus, S. (Ed.), NOAA Atlas NESDIS 64, U.S. Gov. Printing Office, Washington, D.C., 396 pp., CD-ROM.
Garside, C., Garside, J.C., Keller, M.D., Sieracki, M.E., 1996. The formation of high nutrient-low salinity water in the Gulf of Maine: a nutrient trap? Estuarine Coastal Shelf Sci. 42 (5), 617–628.
Goovaerts, P., 1997. Geostatistics for Natural Resource Evaluation, Oxford University Press, New York, NY.
Greene, C.H., Pershing, A.J., 2003. The flip-side of the North Atlantic Oscillation and modal shifts in slope-water circulation patterns. Limnol. Oceanogr. 48, 319–322.
Hopkins, T.S., Garfield III, N., 1979. Gulf of Maine intermediate water. J. Mar. Res. 37, 103–139.
Ji, R., Davis, C., Chen, C., Townsend, D.W., Mountain, D., Beardsley, R., 2008. Modeling the influence of low-salinity water inflow on winter–spring phytoplankton dynamics in the Nova Scotian Shelf – Gulf of Maine region. J. Plankton Res. 30 (12), 1399–1416.
Johnson, D.R., Boyer, T.P., Garcia, H.E., Locarini, R.A., Baranova, O.K., Zweng, M.M., 2009. World Ocean Database 2009 Documentation. Levitus, S. (Ed.). NODC Internal Report 20, NOAA Printing Office, Silver Spring, MD, 175pp.
Kolber, Z., Wyman, K.D., Falkowski, P.G., 1990. Natural variability in photosynthetic energy conversion efficiency: a field study in the Gulf of Maine. Limnol. Oceanogr. 35 (1), 72–79.
Krige, D.G., 1951. A statistical approach to some basic mine valuation problems on the Witwatersrand. J. Chem., Metal. and Mining Soc. South Africa 52 (6), 119–139.
Loder, J.W., 1980. Topographic rectification of tidal currents on the side of Georges Bank. J. Phys. Oceanogr. 10, 1399–1416.
Lynch, D., McGillicuddy, D.M., 2001. Objective analysis for coastal regimes. Cont. Shelf Res. 21 (11–12), 1299–1315.
Matheron, G., 1963. Principles of geostatistics. Econ. Geol. 58, 1246–1266.
Matheron, G., 1969. Le Krigeage Universel. Les Cahiers du Centre de Morphologie Mathématique de Fontainbleau, Fascicule 1.
Matheron, G., 1965. Les Variables Regionalisees et Leur Estimation. Masson, Paris, France.
Meng, Q., Borders, B., Madden, M., 2010. High resolution satellite image fusion using regression kriging. Int. J. Remote Sensing 31 (7), 1857–1876.
Mountain, D.G., 2004. Variability of the water properties in NAFO Subareas 5 and 6 during the 1990s. J. Northwest Atlantic Fish. Sci. 34, 101–110.
Mountain, D.G., 2012. Labrador slope water entering the Gulf of Maine – respons to the North Atlantic Oscillation. Cont. Shelf Res. 47, 150–155.
Mountain, D.G., Jessen, P.F., 1987. Bottom waters of the Gulf of Maine 1978–1983. J. Mar. Res. 45 (2), 319–345.
Myers, D.E., 1989. To be or not to be…stationary? That is the question. Math. Geol. 21 (3), 347–362.
Naimie, C.E., 1996. Georges Bank residual circulation during weak and strong stratification periods: prognostic numerical model results. J. Geophys. Res. 101 (C3), 6469–6486.
Petrie, B., Yeats, P., Strain, P., 1999. Nitrate, silicate, and phosphate atlas for the Scotian Shelf and Gulf of Maine. Can. Tech. Rep. Hydrogr. Ocean Sci. 203 (vii), 96.
Petrie, B., Dean-Moore, J., 1996. Temporal and spatial scales of variability of temperature and salinity on the Scotian Shelf. Canadian Technical Report of Hydrography and Ocean Science 177.
Petrie, B., Yeats, P., 2000. Annual and interannual variability of nutrients and their estimated fluxes in the Scotian Shelf-Gulf of Maine region. Can. J. Fish. Aquat. Sci. 57, 2536–2546.
Pettigrew, N.R., Churchill, J.H., Janzen, C.D., Mangum, L.J., Signell, R.P., Thomas, A.C., Townsend, D.W., Wallinga, J.P., Xue, H., 2005. The kinematic and hydrographic structure of the Gulf of Maine Coastal Current. Deep-Sea Res. II 52, 2369–2391.
Rohde, R., Muller, R., Jacobsen, R., Perlmutter, S., Rosenfeld, A., et al., 2013. Berkeley earth temperature averaging process. Geoinf. Geostat.: An Overview 1, 2.
Roworth, E., Signell, R., 1999. Construction of digital bathymetry for the Gulf of Maine. U.S. Geological Survey Open-File Report 98-801. CD-ROM.

Schlitz, R.J., Cohen, E.B., 1984. A nitrogen budget for the Gulf of Maine and Georges Bank. Biol. Oceanogr. 3, 203–222.
Sherman, K., 1980. MARMAP, a fisheries ecosystem study in the Northwest Atlantic: fluctuations in ichthyoplankton–zooplankton components and their potential for impact on the system. In: Diemer, F.P., Vernberg, F.J., Mirkes, D.R. (Eds.), Advanced Concepts in Ocean Measurements for Marine Biology. Belle W. Baruch Institute for Marine Biology and Coastal Research. University of South Carolina Press, Columbia, South Carolina, pp. 9–37.
Sibunka, J.D., Silverman, M.J., 1984. MARMAP surveys of the continental shelf from Cape Hatteras, North Carolina, to Cape Sable, Nova Scotia (1977–1983). Atlas no. 1. Summary of operations. NOAA Technical Memorandum NMFS-F/NEC-33. 360p.
Smith, P.C., Houghton, R.W., Fairbanks, R.G., Mountain, D.G., 2001. Interannual variability of boundary fluxes and water mass properties in the Gulf of Maine and on Georges Bank: 1993–1997. Deep-Sea Res. Part II 48 (1-3), 37–70.
Song, H., Ji, R., Stock, C., Wang, Z., 2010. Phenology of phytoplankton blooms in the Nova Scotian Shelf-Gulf of Maine region: remote sensing and modeling analysis. J. Phytoplankton Res. 32 (11), 1485–1499.
Song, H., Ji, R., Stock, C., Kearney, K., Wang, Z., 2011. Interannual variability of phytoplankton bloom and plankton productivity in the Nova Scotian Shelf and Gulf of Maine. Mar. Ecol. Prog. Ser. 426, 105–118.
Smith, P.C., 1983. Mean and seasonal circulation off southwest Nova Scotia. J. Phys. Oceanogr. 13, 1034–1054.
Therriault, J.C., Petrie, B., Pepin, P., Gagnon, J., Gregory, D., Helbig, J., Herman, A., Lefaivre, D., Mitchell, M., Pelchat, B., Runge, J., Sameoto, D., 1998. Proposal for a Northwest Atlantic zonal monitoring program. Can. Tech. Rep. Hydrogr. Ocean Sci. 194, 57.
Thomas, A.C., Townsend, D.W., Weatherbee, R., 2003. Satellite-measured phytoplankton variability in the Gulf of Maine. Cont. Shelf Res. 23, 971–989.
Townsend, D.W., 1998. Sources and cycling of nitrogen in the Gulf of Maine. J. Mar. Syst. 16, 283–295.
Townsend, D.W., Pettigrew, N.R., 1997. Nitrogen limitation of secondary production on Georges Bank. J. Plankton Res. 19, 221–235.
Townsend, D.W., Pettigrew, N.R., Thomas, A.C., 2005. On the nature of Alexandrium fundyense blooms in the Gulf of Maine. Deep Sea Res. II 52, 2603–2630.
Townsend, D.W., McGillicuddy, D.J., Thomas, M.A., Rebuck, N.D., 2014. Nutrients and water masses in the Gulf of Maine–Georges Bank region: variability and importance to blooms of the toxic dinoflagellate *Alexandrium fundyense*. Deep-Sea Res. II 103, 238–263.
Townsend, D.W., Thomas, A.C., Mayer, L.M., Thomas, M., Quinlan, J., 2006. Oceanography of the Northwest Atlantic Continental Shelf. In: Robinson, A.R., Brink, K.H. (Eds.), The Sea, vol. 14. Harvard University Press, pp. 119–168.
Townsend, D.W., Ellis, W.G., 2010. Primary production and nutrient cycling on the Northwest Atlantic continental shelf. In: Liu, K.K., Atkinson, L., Quinones, R., Talaue-McManus, L. (Eds.), Carbon and Nutrient Fluxes in Continental Margins: A Global Synthesis. IGBP Book Series. Springer, Berlin, pp. 234–248.
Townsend, D.W., Rebuck, N.D., Thomas, M.A., Karp-Boss, L., Gettings, R.M., 2010. A changing nutrient regime in the Gulf of Maine. Cont. Shelf Res. 20, 820–832.
Xue, H., Chai, F., Pettigrew, N.R., 2000. A model study of the seasonal circulation in the Gulf of Maine. J. Phys. Oceanogr. 30, 1111–1135.
Werme, C., Rex, A.C., Hall, M.P., Keay, K.E., Leo, W.S., Mickelson, M.J., Libby, S., Hunt, C.D., 2012. 2011 outfall monitoring overview. Boston: Massachusetts Water Resources Authority, Report 2012–2011, 62p.
Wiebe, P.H., Beardsley, R.C., Mountain, D.G., Bucklin, A., 1996. Global Ocean Ecosystem Dynamics – initial program in northwest Atlantic. Northwest Atlantic Sea Technol. 37 (8), 67–76.